Differences in the Endosomal Distributions of the Two Mannose 6-Phosphate Receptors

Judith Klumperman,* Annette Hille,‡ Tineke Veenendaal,* Viola Oorschot,* Willem Stoorvogel,* Kurt von Figura,‡ Hans J. Geuze*

*Department of Cell Biology, Center for Electronmicroscopy, Utrecht University, AZU HO2.314, 3584 CX Utrecht, The Netherlands; and ‡Department of Biochemistry, Georg August Universität, 3400 Göttingen, Germany

Abstract. Multiple immunolabeling of cryosections was performed to compare the subcellular distributions of the two mannose 6-phosphate receptors (MPRs) involved in the intracellular targeting of lysosomal enzymes: the cation-dependent (CD) and cation-independent (CI) MPR. In two cell types, the human hepatoma cell line HepG2 and BHK cells double transfected with cDNA's encoding for the human CD-MPR and CI-MPR, we found the two receptors at the same sites: the *trans*-Golgi reticulum (TGR), endosomes, electron-dense cytoplasmic vesicles, and the plasma membrane. In the TGR the two receptors colocalized and were concentrated to the same extent in the same HA I-adaptor positive coated buds and vesicles. Endosomes were identified by the presence of exogenous tracers. The two MPR codistributed to the same endosomes, but semiquantitative analysis showed a relative enrichment of the CI-MPR in endosomes containing many internal vesicles. Two endosomal subcompartments were discerned, the central vacuole and the associated tubules and vesicles (ATV). We found an enrichment of CD-MPR over CI-MPR in the ATV. Lateral segregation of the two receptors within the plane of membranes was also detected on isolated organelles. Double immunolabeling for the CD-MPR and the asialoglycoprotein receptor, which mainly recycles between endosomes and the plasma membrane, revealed that these two receptors were concentrated in different subpopulations of endosomal ATV. The small GTP-binding protein rab4, which has been shown to mediate recycling from endosomes to the plasma membrane, was localized at the cytosolic face of many endosomal ATV. Quantitative analysis of double-immunolabeled cells revealed only a limited codistribution of the MPRs and rab4 in ATV. These data suggest that the two MPRs exit the TGR via the same coated vesicles, but that upon arrival in the endosomes CD-MPR is more rapidly than CI-MPR, segregated into ATV which probably are destined to recycle MPRs to TGR.

At an early stage in their biosynthesis, soluble lysosomal enzymes become selectively phosphorylated on specific mannose residues. This provides the enzymes with a signal that is recognized by mannose 6-phosphate receptors (MPRs)[1], which encounter their ligands in the *trans*-Golgi reticulum (TGR) (Duncan and Kornfeld, 1988) and mediate their targeting to lysosomes. Two distinct MPRs have been identified. The first was discovered by Sahagian et al. (1981), and is now generally referred to as the cation-independent MPR (CI-MPR). It has an apparent molecular mass of ~300 kD and is identical to the type II insulin-like growth factor receptor (Kiess et al., 1988; Morgan et al., 1987). The involvement of the CI-MPR in the translocation of newly synthesized lysosomal enzymes to lysosomes has been well established (for review see Kornfeld and Mellman, 1989). The second receptor is a homodimer of 46 kD (Hoflack and Kornfeld, 1985*a*), which is now often referred to as the cation-dependent MPR (CD-MPR), because ligand binding is improved by the presence of divalent cations at certain conditions (Hoflack and Kornfeld, 1985*a*,*b*; Junghans et al., 1988; Watanabe et al., 1990). Like the CI-MPR, the CD-MPR is involved in the targeting of lysosomal enzymes to lysosomes (Braulke et al., 1988; Stein et al., 1987*a*). Both receptors bind phosphorylated oligosaccharides at a slightly acidic pH and release their ligands at pH 5.5 or less (Hoflack et al., 1987; Tong and Kornfeld, 1989).

Binding to their receptors prevents lysosomal enzymes from being secreted. Instead, they are selectively segregated into clathrin-coated areas of the TGR, which form vesicles which are destined for fusion with endosomes. This process is mediated by an oligomeric protein complex present in the coats, the HA I-adaptor, which binds to the cytosolic tail of

J. Klumperman's present address is Graduate School Neurosciences Amsterdam, Vrije University, Faculty of Biology, Boelelaan 1087, 1081 HV Amsterdam, The Netherlands.

1. *Abbreviations used in this paper*: ASGPR, asialoglycoprotein receptor; ATV, associated tubules and vesicles; CD-MPR, cation-dependent MPR; CI-MPR, cation-independent MPR; mannose 6-phosphate receptor; Tf-HRP, transferrin-HRP; TGR, *trans*-Golgi reticulum.

the CI-MPR (Glickman et al., 1989). After being transported to endosomes, ligands dissociate from their receptor due to the acidic environment, after which the MPRs recycle to the TGR or plasma membrane and lysosomal enzymes are incorporated into lysosomes (Brown et al., 1985; Jin et al., 1989; Goda and Pfeffer, 1988). Exogenous lysosomal enzymes carrying mannose 6-phosphate can bind to the CI-MPR at the cell surface and be delivered to lysosomes via the endocytotic pathway (for review see Kornfeld and Mellman, 1989). In contrast to the CI-MPR, the CD-MPR is not able to bind lysosomal enzymes at the cell surface and hence does not participate in the endocytosis of lysosomal enzymes (Stein et al., 1987*a*).

Although the CD-MPR has been implicated to mediate the transport of lysosomal enzymes from the TGR to endosomes, Chao et al. (1990) reported a finding that indicated an additional, unexpected, function of the CD-MPR. Transfection of BHK and mouse L cells with cDNA encoding the human CD-MPR leads to the enhanced secretion of newly synthesized lysosomal enzymes. Two possible pathways were postulated to explain the mechanism which enables the CD-MPR to deliver ligands to both lysosomes and the extracellular environment. The CD-MPR may accompany its ligand all the way to the plasma membrane where ligand dissociation is induced by the external milieu. Alternatively, the CD-MPR–ligand complexes may dissociate within early endosomes after which free ligands could reach the cell surface by incorporation into vesicles that bud from the early endosome and fuse with the plasma membrane. The latter hypothesis could imply that the two receptors deliver their ligands either to the same endosomes, and that ligand dissociation occurs at different stages of the endosomal pathway, or that the two types of MPR deliver their ligands to different subsets of endosomes.

The functional differences between the two MPRs may be reflected in differential steady-state distributions of the two receptors. Two previous immunocytochemical studies failed to reveal such differences, probably because of the low expression levels of CD-MPR (Bleekemolen et al., 1988) or the inability to simultaneously immunolabel for the CD-MPR and CI-MPR at the electronmicroscopical level (Matovcik et al., 1990). Using HepG2 cells containing sufficient CD-MPR to perform colocalization with CI-MPR and BHK cells transfected with the human cDNAs for both receptors, we demonstrate that the two receptors exit the TGR via the same, HA I-decorated vesicles, and codistribute to the same population of endosomes. However, within endosomes the CD-MPR is more concentrated in the electron-dense tubules and vesicles (ATV) that are associated with the vacuolar part of the endosome, suggesting a higher rate of retrieval of CD-MPR from the maturing endosome. Double immunolabeling of the two MPR with markers that putatively labeled ATV traveling from endosomes to the plasma membrane, the asialoglycoprotein receptor and rab4, revealed only limiting co-localization, suggesting that MPR localize to a distinct population of endosomal ATV.

Materials and Methods

Materials

The human hepatoma cell line HepG2, clone A16, was cultured as described (Stoorvogel et al., 1987). BHK cells co-expressing the human CD-MPR (average level of overexpression: 49×) and CI-MPR (average level of overexpression: 60×) were generated as described by Chao et al. (1990). The transferrin-HRP (Tf-HRP) conjugate was prepared and analyzed as reported by Stoorvogel et al. (1988, 1991). Protein A-gold was prepared as described (Slot et al., 1988). Complexation of BSA with 5 nm gold was performed via the same procedure. BSA was dissolved in distilled water and dialyzed overnight against distilled water before use. The BSA-gold complex was concentrated and stored at 4°C until use. The optical density of the gold probe at a wavelength of 520 nm was adjusted to 10. Before applying the BSA-gold to the cells it was dialyzed overnight against MEM, 20 mM Hepes-NaOH, pH 7.2 (MEMH).

Uptake of Endocytotic Markers

The endosomal pathway in HepG2 cells was marked by the presence of internalized Tf-HRP. We choose this marker, because HepG2 cells internalize only trace amounts of BSA-gold (see below). HepG2 cells grown on 6-cm petri dishes (Costar, Badhoevedorp, The Netherlands) were incubated in a 37°C waterbath for either 5 or 20 min in 1.5 ml MEMH containing 25 μg/ml Tf-HRP. The uptake of ligand was stopped by the addition of 1.5 ml 4% glutaraldehyde in 0.1 M phosphate buffer, pH 7.4. After 3 h at room temperature the cells were scraped, washed 3 times with PBS at pH 7.4, and stored until processing for cryo-ultramicrotomy.

In contrast to HepG2 cells BHK cells internalized large amounts of BSA-gold, which therefore was chosen as an appropriate marker of the endosomal pathway in these cells. Subconfluent BHK cells cultured on 6-cm petri dishes (Greiner, Alphen a/d Rijn, The Netherlands) were incubated with 1.5 ml of BSA-gold containing medium for 3, 5, or 90 min in a 37°C waterbath. The uptake was stopped by washing the cells with ice-cold 0.1 M phosphate buffer, pH 7.4, until no gold could be detected in the buffer. Subsequently the cells were fixed for 2 h at room temperature with a mixture of 0.1% glutaraldehyde (Polysciences Inc., Warrington, PA) and 1% acrolein (BDH Chemicals LTD Poole, England) in 0.1 M phosphate buffer, pH 7.4, after which the cells were rinsed three times with PBS pH 7.4 and stored until processing for cryo-ultramicrotomy.

Antibodies

The CD-MPR was immunolocalized with a mAb raised against human CD-MPR (10C6; A. Hille, unpublished observation) or with an affinity-purified rabbit antibody (MSCI), raised against the cytosolic tail of human CD-MPR (Schulze-Garg, C., and A. Hille, manuscript in preparation). Both antibodies gave identical labeling patterns. To immunolocalize the CI-MPR in homogenates of HepG2 cells we used an antibody generated against a synthetic peptide representing amino acids 2048–2660 of the cytosolic tail of the rat CI-MPR, which was kindly provided by G. Lienhard (Dartmouth Medical School, Hanover, NH). To immunolocalize the CI-MPR in cryosections we used affinity-purified rabbit anti-human CI-MPR (Geuze et al., 1985). The specificity of the labeling was confirmed in BHK cells that were not transfected for either MPR and in which immunolabeling with the anti-human MPR yielded virtually no gold label (not shown). Rabbit anti-HRP was purchased from Sigma Immunochemicals (St. Louis, MO). Anti-human asialoglycoprotein receptor (ASGPR) has been described by Geuze et al. (1983, 1984). On isolated organelles the ASGPR was monitored using a mouse IgG1 mAb (4F1), which specifically recognizes the cytoplasmic tail of the H1 subunit of the human ASGPR on Western blots and by immunoprecipitation (not shown). These interactions could be inhibited by the addition of excess synthetic peptide comprising the first 17 amino acids of the ASGPR H1 polypeptide. The antibody against the γ adaptin of the HA I complex has been described (Ahle et al., 1988). Rabbit anti-rab4 was a kind gift of Dr. B. Goud (Institut Pasteur, Paris, France).

Processing for Electronmicroscopy

Control cells were fixed with a mixture of 0.2% glutaraldehyde and 2% acrolein in 0.1 M phosphate buffer, pH 7.4, that was added to an equal volume of culture medium. After 2 h at room temperature the cells were rinsed 3 times with PBS and stored until further processing. In case of immunolabeling with anti-ASGPR the cells were fixed in 2% formaldehyde (Merck, Darmstadt, Germany) in 0.1 M phosphate buffer during 16 h. Higher concentrations of formaldehyde or the addition of glutaraldehyde or acrolein abolished the labeling. Rab4 could be localized when cells were fixed in the glutaraldehyde/acrolein mixture or in 2% glutaraldehyde in 0.1 M phosphate buffer.

Fixed cells were scraped with a rubber policeman and washed 3 times with 0.15% glycine in PBS. Then the cells were resuspended in 10% gelatine in PBS, which was cut into 1-mm^3 squares at 4°C. These blocks were impregnated with 2.3 M sucrose at 4°C for a least 2 h and frozen in liquid nitrogen. Cryosections were prepared and single, double, or triple immunolabeled as described (Slot et al., 1988, 1991).

Semi-quantitative Immuno-electronmicroscopy

The distribution patterns of the CD-MPR and CI-MPR over the various compartments of HepG2 cells were established in a semi-quantitative manner. We selected areas of the grids that contained cells exhibiting a good overall ultrastructure. These areas were scanned along a fixed track. Gold particles within a distance of 30 nm from a membrane were counted as positive. Nonspecific labeling, measured over the nuclei, amounted 1 gold particle per 4.3 μm^2 for anti-CD-MPR antibody 10C6, 1 gold particle per 6.45 μm^2 for anti-CD-MPR antibody MSCI and 1 gold particle per 19 μm^2 for anti-CI-MPR. These values were considered neglectable. All quantitations in HepG2 cells were performed in triple-immunolabeled cells, allowing a direct comparison of the CD-MPR, the CI-MPR, and internalized Tf-HRP, and performed on at least two different grids. Quantitation of the distribution pattern of the two MPRs in BHK cells was performed in a similar way, using BSA-gold as an endocytotic marker. Because of the high labeling intensity of the two MPRs in the double-transfected BHK cells quantitations were performed on single immunolabeled cells.

Preparation and Immunolabeling of Cell Homogenates on Nitrocellulose

HepG2 cells grown in 6-cm culture dishes were washed three times with MEMH, followed by a 30-min incubation in MEMH in a 37°C waterbath. After, having depleted the transferrin receptors from their ligands, the cells were incubated for 30 min at 37°C in MEMH supplemented with 25 μg/ml Tf-HRP. Excess ligand was removed by four washes in ice-cold MEMH. Tf-HRP bound to receptors at the plasma membrane was removed by 10-min incubations at pH 4.5 (150 mM NaCl, 50 μM desferrioxamine, 2 mM $CaCl_2$, 25 mM Na-acetate/acetic acid, pH 4.5) and MEMH, respectively (Stoorvogel et al., 1991). After ligand internalization and removal of extracellular ligand, the cells were washed with, scraped, and homogenized in homogenization buffer (0.25 M sucrose, 1 mM EDTA, 1 mM PMSF, 10 mM Hepes/NaOH, pH 7.2) by passing them 10 times through a 30-gauge syringe. After a 10-min centrifugation at 350 g 100-μl samples of the postnuclear supernatant were applied to 0.4 μm nitrocellulose paper which was placed in a dot-blot apparatus. After pulling the samples through the nitrocellulose under mild vacuum, adhered proteins and organelles were fixed in 2% glutaraldehyde in 0.1 M phosphate buffer, pH 7.4, for 60 min at room temperature. After a 30-min wash with 0.1 M phosphate buffer the filters were incubated 30 min at room temperature in 0.1 M phosphate buffer, pH 7.4, containing 1 mg/ml 3,3'-diaminobenzidine and 0.02% H_2O_2. The nitrocellulose spots were cut out and transferred to PBS. Handling of the filters occurred by placing them in eppendorf vials containing

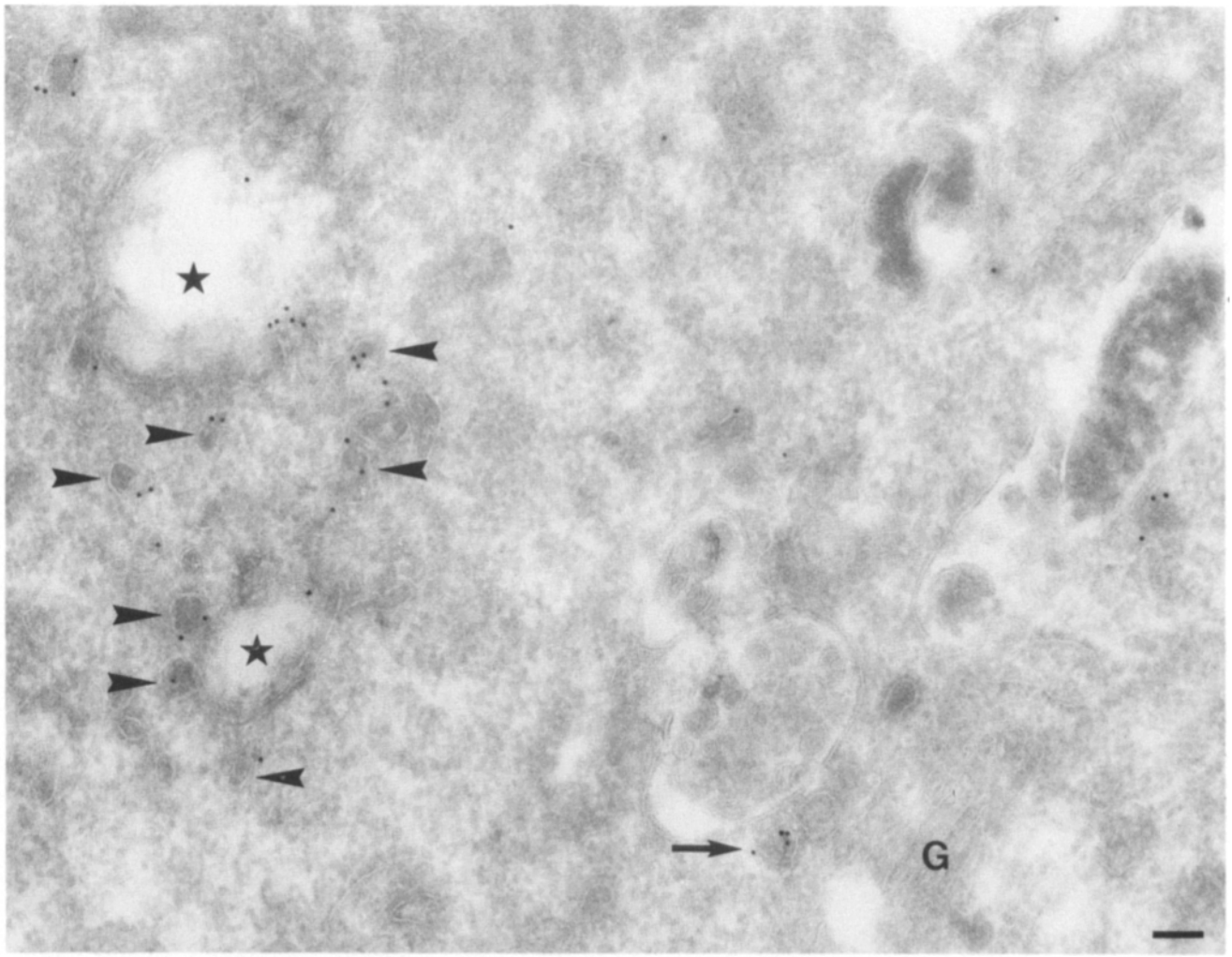

Figure 1. Overview of the immunogold labeling achieved for the CD-MPR in control HepG2 cells. Label is present in a profile (*arrow*) near a Golgi complex (*G*) and in both the central vacuole (★) and the associated electron-dense tubules and vesicles (*arrowheads*) of endosomes. Bar, 0.1 μm.

the appropriate buffers. First the filters were incubated three times 5 min with PBS/0.15% glycine and once for 45 min with PBS/1% BSA. Next the filters were incubated for 60 min in PBS containing the first antibody that was directed against the cytoplasmic tail of the CD-MPR, CI-MPR, or ASGPR. Excess of antibody was removed with three washes of 5 min each with PBS/0.1% BSA. Filterbound antibodies were labeled with protein A-gold for 20 min, after which the surplus of nonbound protein A-gold was washed away with PBS (three times 5 min). Anti-ASGPR was detected by using a rabbit anti-mouse IgG polyclonal antiserum before the protein A-gold incubation. Subsequently the filters were fixed 20 min in PBS containing 2% glutaraldehyde. After incubations for 5 min in PBS and three times 5 min in PBS/0.15% glycine the filters were labeled with a second antibody followed by protein A-gold particles of a different size than used for the first antibody. Labeling efficiencies were independent of the sequence of incubation with the anti-receptor antibodies. Finally the filters were impregnated with 2% agar in aqua dest and postfixed in 2% glutaraldehyde in 0.1 M Na-cacodylate for 30 min at room temperature. After three washes with 0.1 M Na-cacodylate a final fixation of 30 min with 1% OsO_4 in 0.1 M Na-cacodylate was performed. The filters were embedded in Epon as described (Klumperman et al., 1990).

Results

Subcellular Localization of the CD-MPR and the CI-MPR in HepG2 Cells

Immunolabeling of the CD-MPR in cryosections of HepG2 cells yielded a specific labeling pattern (Fig. 1). Like the CI-MPR (Geuze et al., 1985), the CD-MPR was localized to the TGR, endosomes, cytoplasmic vesicles, and at the plasma membrane. TGR elements were recognized by their characteristic morphology (Geuze et al., 1985, 1993), their proximity to the Golgi stack and the absence of internalized Tf-HRP. The types of membranes that following these criteria were defined as TGR provided the principal sites of label for the Golgi adaptor HA I (see below). Both CD-MPR and CI-MPR were found in coated and noncoated membranes of the TGR, while label over the Golgi cisternae was low (Fig. 2).

To make a distinction between early and late endosomes we tried to correlate the ultrastructural diversity of the MPR containing endosomes with a putative time-dependent appearance of internalized Tf-HRP. However, already after 5 min of uptake Tf-HRP was detected in all types of MPR containing endosomes (data not shown, see also Stoorvogel et al., 1991). We therefore used morphological criteria to discern two subsets of endosomes. Endosomes containing MPR consisted of a central vacuolar element and associated tubules. The lumen of the central vacuoles contained various numbers of internal vesicles (Fig. 3, *B–F*). The numbers of internal vesicles are considered to indicate the developmental stage of endosomes along the endocytotic pathway since these vesicles accumulate upon maturation (Hopkins et al., 1990; Klumperman et al., 1990; Slot et al., 1991; Stoorvogel et al., 1991; van Deurs, B., personal communication). We distinguished "early" endosomes with up to three internal vesicles in the central vacuole (Fig. 3, *A–D*) and "late" endosomes of which the central vacuole carried many internal vesicles (Fig. 3, *E* and *F*). Membrane continuities between the central vacuole and the associated tubules are shown in Fig. 3, *B* and *F*, but usually the tubules appeared as electron dense vesicles in close proximity to the central vacuole. Since we could not discriminate between endosome-associated tubules in cross section and free vesicles we designated this part of the endosomal complex as "associated tubules and vesicles" (ATV). Fig. 3 shows that both MPRs were found in the central vacuole and in the ATV.

Both receptors were also found in typical, small, electron-dense vesicles located throughout the cytoplasm. The vesicles were ~90 nm in diameter, they did not bear an electron-dense coat, and were devoid of label for Tf-HRP. Morphologically they resembled the endosomal ATV, but at least in the plane of the section, they were not associated with endosomes. Therefore we called these vesicles "cytoplasmic vesicles."

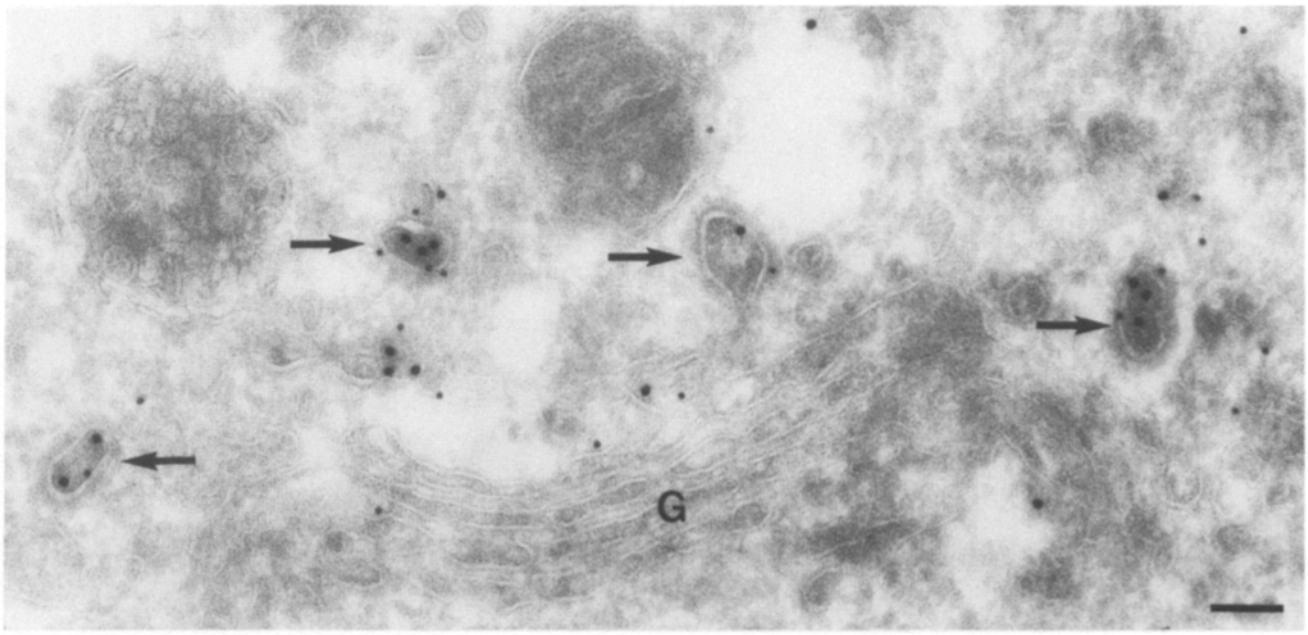

Figure 2. Double immunolabeling of the CD-MPR (10 nm gold) and the CI-MPR (15 nm gold) in the TGR of HepG2 cells. The two receptor types colocalize both in noncoated and coated (*arrows*) regions of the TGR. Label over the Golgi-stack (*G*) is only low. Bar, 0.1 μm.

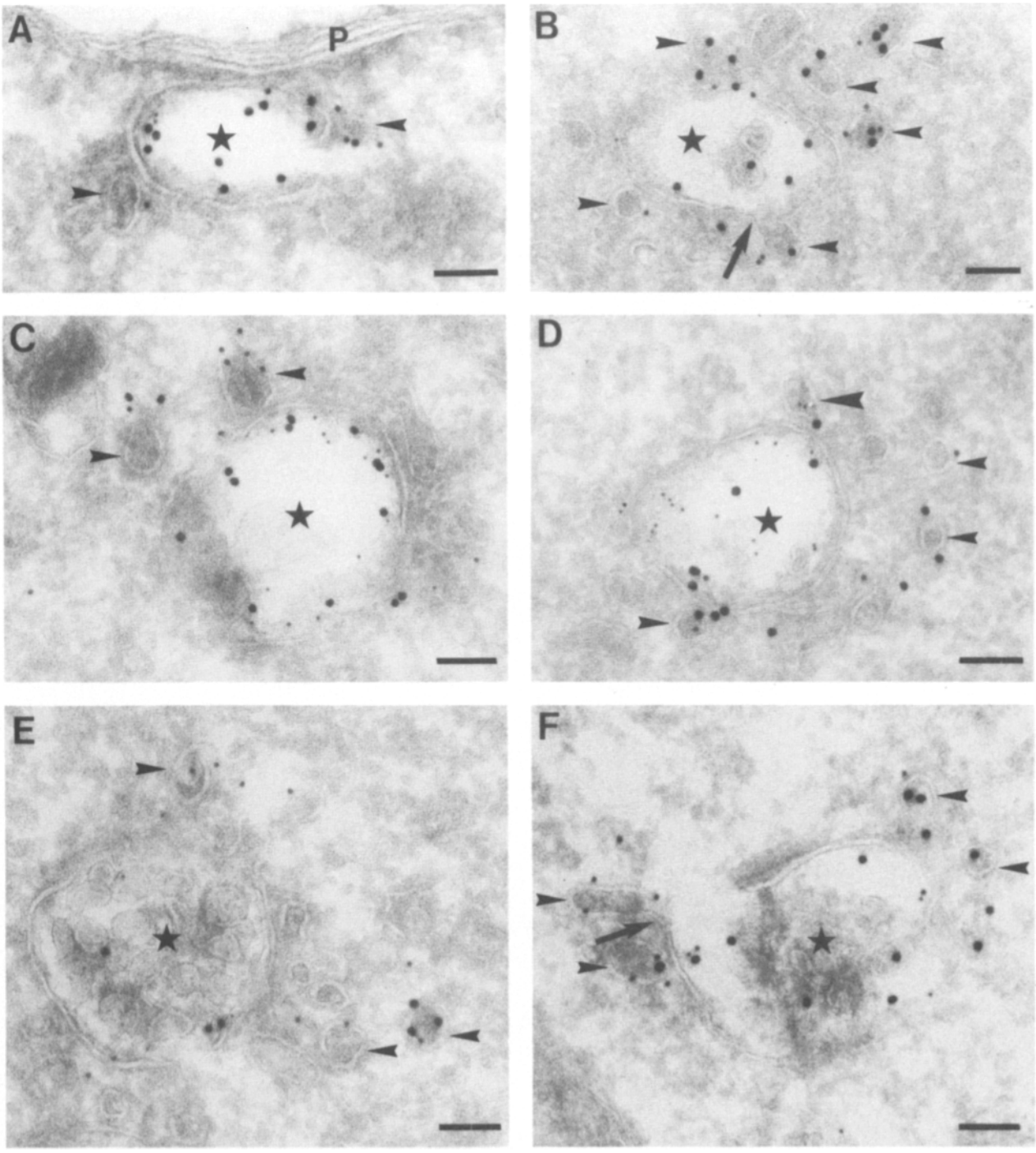

Figure 3. Triple immunolabeling of internalized Tf-HRP (5 nm gold), the CD-MPR (10 nm gold), and the CI-MPR (15 nm gold) in endosomes of HepG2 cells containing various amounts of internal membranes. The endosomes (★) in *A–D* were designated early in *E* and *F* late. Note that both receptors are present in the central vacuole of the endosomal complex as well as in the dense associated tubules and vesicles, the so-called ATV (*small arrowheads*). The arrows in *B* and *F* point to continuities between these two subcompartments. Only occasionally we found Tf-HRP label in the ATV (*D, large arrowhead*). *P*, plasma membrane. Bars, 0.1 μm.

Semi-quantitative Analysis of the Distribution of the CD-MPR and CI-MPR in HepG2 Cells

The relative distribution of the CD-MPR and CI-MPR over the different compartments was assessed in a semi-quantitative manner using cryosections triple immunolabeled for the two receptors and internalized Tf-HRP. The results of this quantitation are presented in Table I. The major site of labeling for both receptors was the TGR, i.e., in Tf-HRP-negative, Golgi-associated, partially coated, membranes: 37.3% of the CD-MPR and 39.6% of the CI-MPR label. Endosomes, i.e., Tf-HRP–positive complexes of central vacuole and ATV, contained 14.3% of CD-MPR and 22.3% of CI-MPR

Table I. Subcellular Distribution of the CD and CI-MPR in Triple-immunolabeled (CD-MPR;CI-MPR;Tf-HRP) Cryosections of HepG2 Cells After 20 Min Tf-HRP Uptake

	Percent CD-MPR ± SEM	Percent CI-MPR ± SEM
TGR	37.3 ± 2.9	39.6 ± 2.5
Golgi Stack	1.9 ± 1.1	1.7 ± 0.9
Early endosomes	7.4 ± 2.1	10.0 ± 2.3
Late endosomes	6.9 ± 1.3	12.3 ± 1.2
Cytoplasmic vesicles	22.7 ± 1.7	11.7 ± 1.6
Plasma membrane and coated pits	5.3 ± 0.3	7.6 ± 0.2
Rest	18.4 ± 2.7	17.1 ± 2.3

The numbers of gold particles over the different cell compartments are expressed as percentage of the totals counted for each MPR and represent the mean of four separate quantifications in different grids. The different categories were defined as described in the text. In total 1,491 gold particles representing the CD-MPR and 2,632 gold particles representing the CI-MPR were encountered.

label. The two MPRs and Tf-HRP colocalized to both early and late endosomes (Fig. 3), but in late endosomes the percentage of CI-MPR label was significantly higher than for the CD-MPR (t test, $p = 0.05$).

Another significant difference was the relative distribution of the label over the cytoplasmic vesicles. Compared with the CI-MPR twice as much CD-MPR label was found in this type of vesicles. Consistent with biochemical data (Stein et al., 1987*b*; Pfeffer et al., 1987) small numbers of the CD-MPR (5.3%) and the CI-MPR (7.6%) were found at the cell surface. Both receptors were detected within the same coated pits, indicating a common path of entry.

Finally, label for both receptors was found over unidentified membranes and over profiles each of which contained <3% of the total label. We collected this label in the category "rest." Presumably part of the unidentified membranes represented TGR which was not classified as such, because the associated Golgi stack was not observed. No differences in labeling for both receptors within this category were detected.

Colocalization of the CD-MPR and CI-MPR in HA I–coated Vesicles of the TGR

The Golgi adaptor HA I has been found to mediate the incorporation of CI-MPR in vesicles destined for transport to endosomes (Glickman et al., 1989). To investigate whether HA I–coated TGR vesicles harbor both MPR species, we triple-immunolabeled sections for HA I, CD-MPR, and CI-MPR. CI-MPR and CD-MPR colocalized in noncoated regions of the TGR and in the same, coated TGR buds and vesicles (Fig. 2), which were HA I positive (Fig. 4). By determining the number of gold particles per membrane length we have previously found that the CI-MPR is concentrated in HA I–coated TGR membranes over noncoated TGR membranes

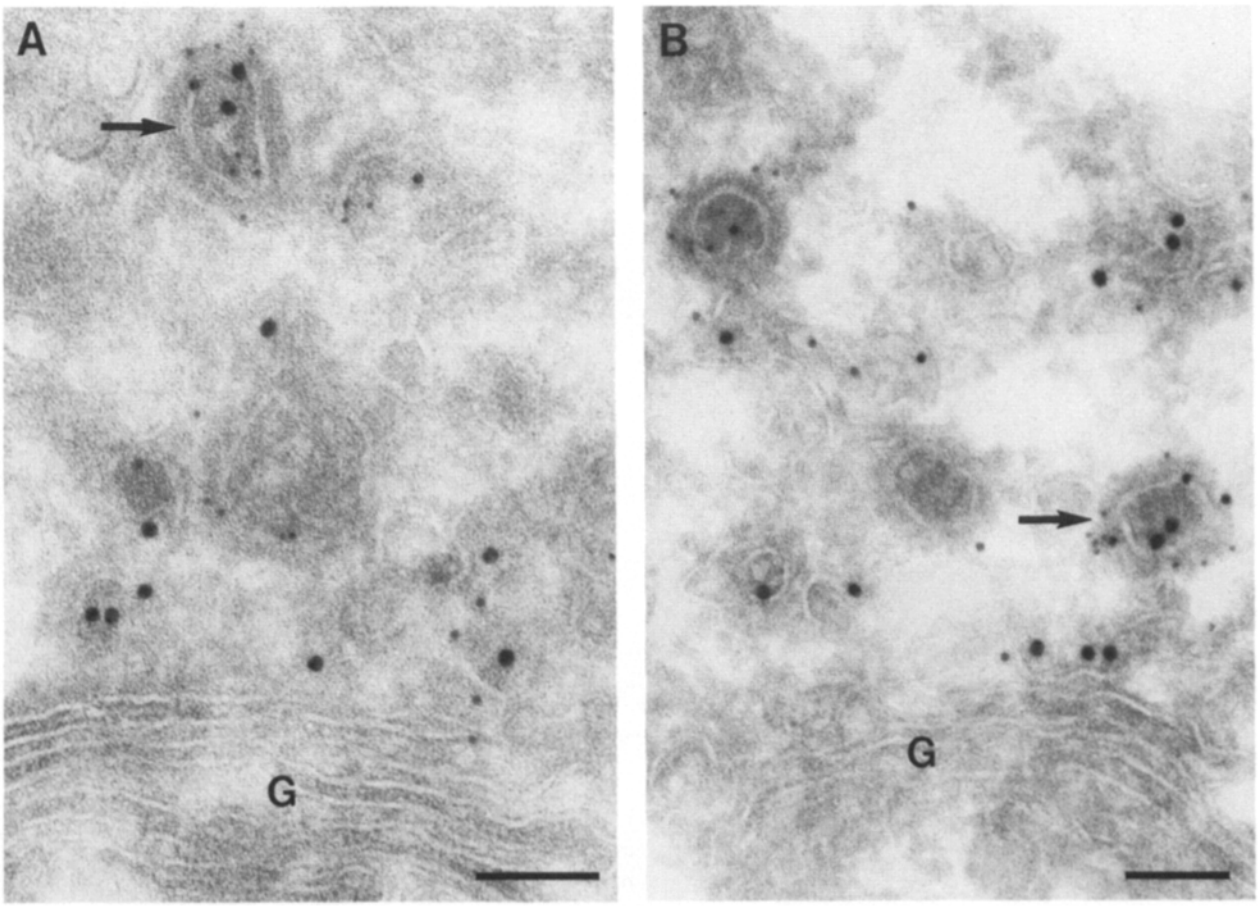

Figure 4. Colocalization of the CD-MPR and CI-MPR in different regions of the TGR of HepG2 cells. A triple immunolabeling was performed by subsequent incubation with antibodies against the adaptor protein HA I (5 nm gold), the CD-MPR (10 nm gold), and the CI-MPR (15 nm gold). The two MPRs colocalize within HA-I coated vesicles (*arrows*). *G*, Golgi complex. Bars, 0.1 μm.

Table II. Relative Distribution of the CD-MPR and CI-MPR in HA I-positive and HA I-negative Membranes of the TGR

TGR area	Percent CD-MRP	Percent CI-MPR
HA I-positive	50.7	50.5
HA I-negative	49.3	49.5

The quantitation was performed in 25 TGR profiles which were identified as tubulo-vesicular compartments in close proximity of a Golgi stack. The numbers of gold particles found over the indicated areas are expressed as percentages of total label within the TGR. In total 142 gold particles representing the CD-MPR and 412 gold particles representing the CI-MPR were counted.

Table III. Relative Distribution of the CD-MPR and CI-MPR Over the Central Vacuole and ATV of Early and Late Endosomes of HepG2 Cells

Type of endosome	Subcompartment	Percent CD-MPR	Percent CI-MPR	Percent CD-MPR/ Percent CI-MPR
Early	Central vacuole	58.5	86.5	0.68
	ATV	41.5	13.5	3.07
Late	Central vacuole	37.9	82.7	0.46
	ATV	62.1	17.3	3.59

Quantitations were performed in cryosections that were triple immunolabeled for the two receptors and internalized Tf-HRP. The numbers of gold particles found over the two endosomal subcompartments are expressed as percentages of the total labeling within early or late endosomes. In total, 99 early and 121 late endosomes were encountered.

of HepG2 cells (Geuze et al., 1992). To study this for the CD-MPR we compared the proportion of the two receptors within coated and noncoated regions of the TGR. As shown in Table II the ratio of CD-MPR over CI-MPR was equal in the coated and noncoated membrane areas of the TGR. Together with our previous results this indicates that both receptors are enriched to the same extent in the HA I-positive TGR membranes, suggesting that these areas provide a common exit site for the two MPRs from the TGR.

Relative Distribution of the CD-MPR and the CI-MPR Over Endosomal Subcompartments

Within endosomes both the CD-MPR and the CI-MPR were found in the central vacuole, as well as in the ATV (Fig. 3). However, the relative distribution of the two receptors over these two subcompartments differed significantly. In early endosomes 41.5% of the CD-MPR was found in the ATV, as compared with 13.5% of the CI-MPR label (Table III). Thus the CD-MPR is enriched over the CI-MPR in ATV by a factor of 3.07. In late endosomes this differential distribution is even more pronounced: 62.1% of the total CD-MPR label was found in the ATV, as compared with 17.3% of the CI-MPR label (relative enrichment of CD-MPR in the ATV: 3.59). When the ratio of CD-MPR over the CI-MPR in the ATV versus that in the central vacuole is calculated the relative enrichment of the CD-MPR is even more obvious, i.e., 4.5 in early and 7.8 in late endosomes. Thus, in the ATV of both early and late endosomes the CD-MPR is enriched over the CI-MPR.

Double-immunolabeling of MPR with ASGPR and Rab4

After retrieval from the endosome, transport of MPR to ei-

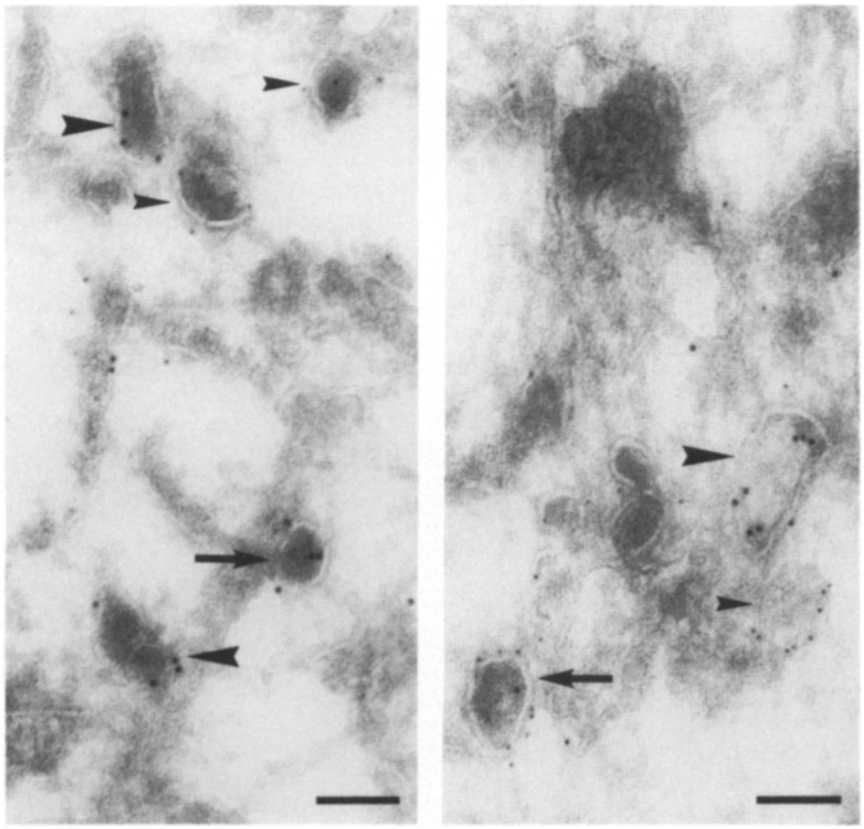

Figure 5. Double immunolabeling of the CD-MPR (5 nm) and the ASGPR (10 nm) in HepG2 cells. Although limited colocalization within the same ATV occurs (*arrows*), the majority of vesicles contain either CD-MPR (*small arrowheads*) or ASGPR (*large arrowheads*). Bars, 0.1 μm.

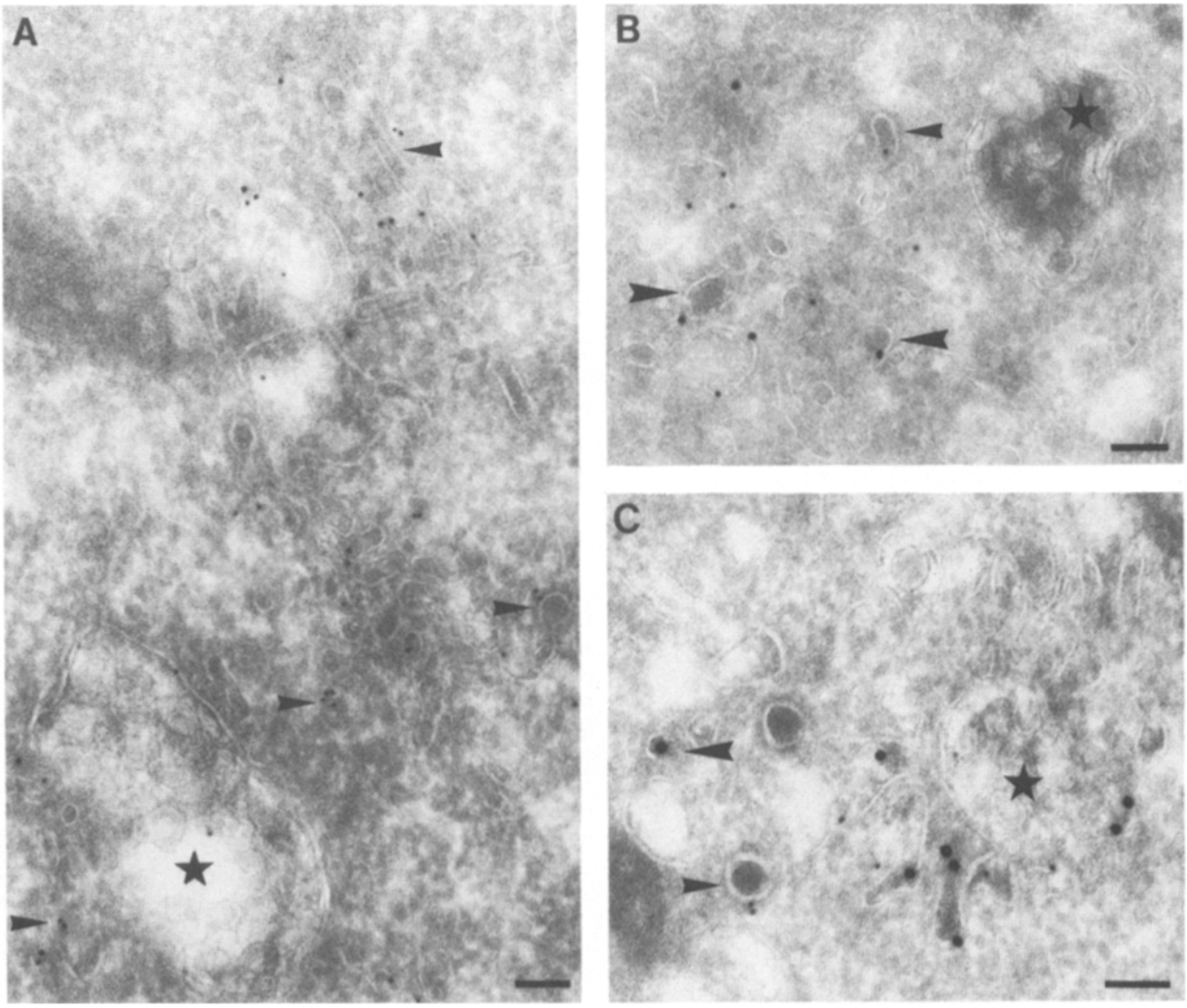

Figure 6. Immunolocalization of rab4 to endosomes (★) of HepG2 cells. (*A*) rab4 (10 nm gold) is mainly associated with endosomal ATV (*arrowheads*). (*B*) Double immunolabeling of rab4 (10 nm gold) and CD-MPR (15 nm gold). (*C*) Double immunolabeling of rab4 (10 nm gold) and CI-MPR (20 nm gold). ATV containing either rab4 (*arrowheads*) or MPR (*large arrowheads*) are indicated. Bars, 0.1 μm.

ther the plasma membrane or the TGR may occur. For both pathways the involvement of endosomal ATV has been proposed (Geuze et al., 1983, 1987, 1988). To discriminate between these two classes of recycling vesicles we labeled HepG2 cells for the ASGPR, known to cycle predominantly between endosomes and the plasma membrane (for review see Schwartz, 1984). We preferred the ASGPR as a marker for this pathway over internalized Tf-HRP, since it resulted in a higher yield of label in the ATV. Double-immunolabeling revealed only limited colocalization of the CD-MPR and ASGPR, most of the label for either receptor being concentrated in separate subpopulations dense vesicles, i.e., endosomal ATV and the cytoplasmic vesicles (Fig. 5).

Recent studies by Van de Sluys et al. (1992) on the regulation of recycling of transferrin receptors by rab4 identified this monomeric GTP-binding protein as another putative marker for recycling vesicles from endosomes to the plasma membrane. Under strong fixation conditions we succeeded to immunolocalize rab4 in HepG2 cells. In agreement with a role in recycling from endosomes, rab4 was found at the cytosolic face of ATV of both early and late endosomes (Fig. 6 *A*). Some of the rab4 containing vesicles were surrounded by an electron-dense coat. Rab4 was not present at the central vacuole of endosomal complexes. Double immunolabeling of rab4 and CD-MPR (Fig. 6 *B*) or rab4 and CI-MPR (Fig. 6 *C*) showed that only occasionally MPR codistributes to rab4 positive endosomal ATV. Quantitative analysis of

Table IV. Relative Distribution of CD-MPR, CI-MPR, and Rab4 in ATV of Early and Late Endosomes

	Type of ATV (Number)	Only rab4 ±SEM	Rab4 and MPR ±SEM	Only MPR ±SEM
CD-MPR	Early (98)	47.7 ± 6	8.3 ± 2.3	44.3 ± 3.5
	Late (119)	50.7 ± 7.5	9.0 ± 2.5	40.3 ± 9.9
CI-MPR	Early (158)	33.7 ± 3.8	14.7 ± 4.1	52.3 ± 2
	Late (116)	41.1 ± 8.4	5.8 ± 3	52.3 ± 8.1

Cryosections of HepG2 cells were double immunolabeled for rab4 and either CD-MPR or CI-MPR and randomly screened for endosomes. Each ATV was classified as in the table. The figures represent percentages (means of three separate quantitations on different grids) of the total number of ATV counted.

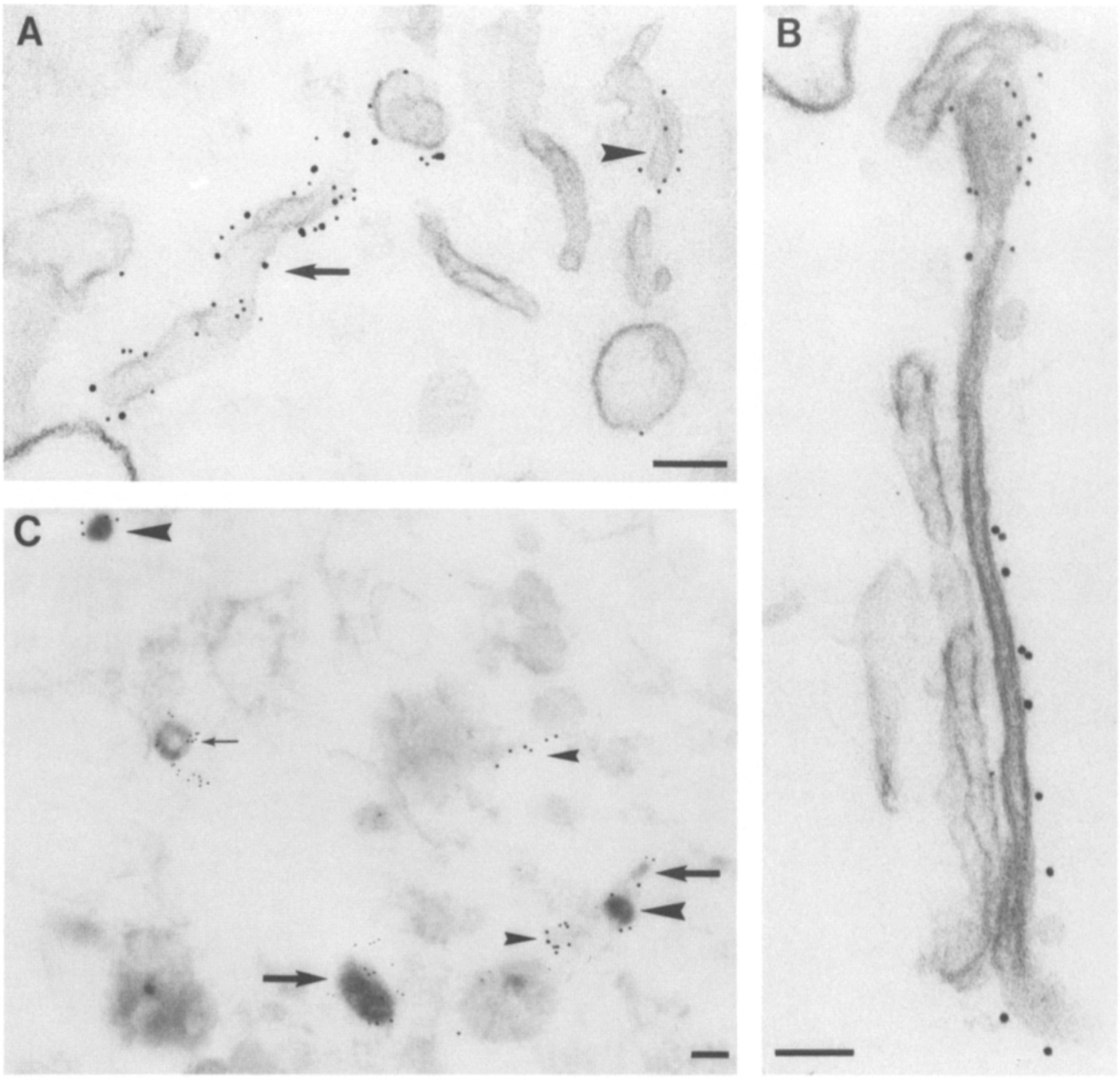

Figure 7. Double immunolabeling of the CD-MPR and CI-MPR (*A* and *B*) and the CD-MPR and ASGPR (*C*) or organelles isolated from HepG2 cells. After 20 min of Tf-HRP internalization postnuclear supernatants were applied to nitrocellulose filters and immunolabeled with antibodies against the cytosolic tails of the respective receptors. The presence of Tf-HRP was visualized by the DAB reaction product. (*A*) CD-MPR 5 nm gold; CI-MPR 10 nm gold. Tf-HRP positive structure (*arrow*) in which the gold label for both MPRs is evenly distributed along the membrane. A vesicle bearing only CD-MPR label is indicated with an arrowhead. (*B*) CD-MPR 10 nm gold; CI-MPR 5 nm gold. Tf-HRP positive structure in which the two MPRs are segregated in the plain of the membrane. (*C*) CD-MPR 10 nm gold; ASGPR 5 nm gold. Most of the Tf-HRP positive structures label for either the CD-MPR (*large arrowheads*) or the ASGPR (*small arrow*). Only a few CD-MPR gold particles colocalize with ASGPR in Tf-HRP positive vesicles (*arrows*). Tf-HRP-negative structures containing CD-MRP only are seen at the small arrowheads. Bars, 0.1 μm.

these labeling patterns revealed the existence of two distinct populations of ATV, with either MPR or rab4 label (Table IV). Unfortunately, the labeling efficiency of the anti-ASGPR antibody in cryosections of cells fixed under conditions needed to visualize rab4 was too low to allow a comparison of the distribution patterns of these two markers.

Together these data show the existence of different subpopulations of endosomal ATV, and that only a minority of MPR is present in ATV that are likely to travel to the plasma membrane.

Immunolabeling of the CD-MPR, CI-MPR, and ASGPR in Isolated Membranes

To further study the distribution of the two MPRs along continuous membranes, we labeled a crude cellular membrane fraction with antibodies against the cytosolic tails of the two receptors. With this method antigenic epitopes in whole membranes can be labeled and not, as in cryosections, only those at the section surface. This leads to a considerable increase in the yield of gold label (Fig. 7). Before fraction-

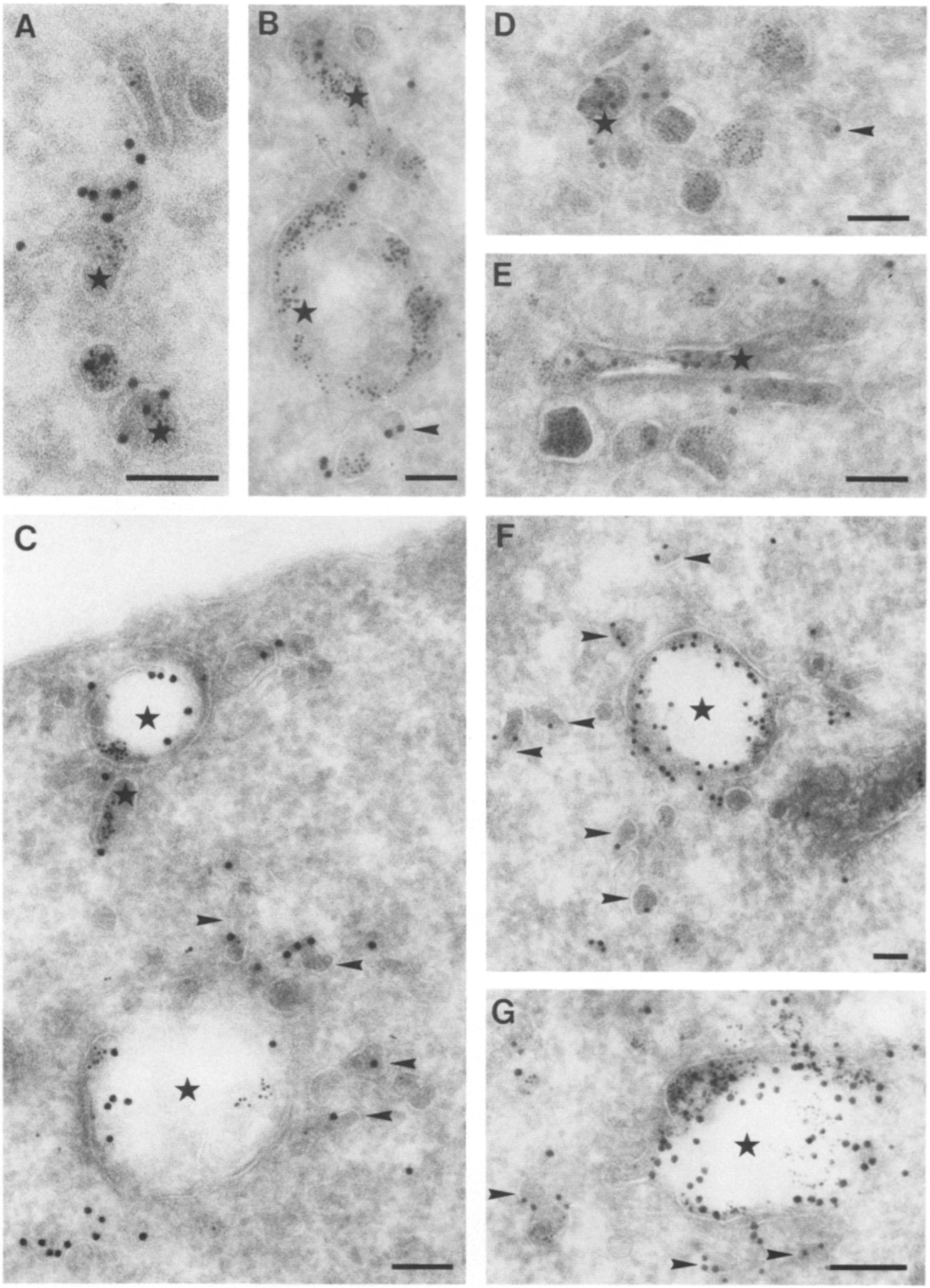

ation, cells were incubated 30 min with Tf-HRP and the electron-dense DAB-reaction product was used as a marker for endosomes.

With antibodies directed against the cytosolic tails of the two MPRs, we obtained an abundant and specific reaction in a variety of membranes, whereas nonspecific labeling of mitochondria for example was very low. Double immunolabeling showed that the majority of MPR-positive structures contained both receptors, with the gold label evenly distributed over the membranes (Fig. 7 *A*). In agreement with our observations in cryosections that the two MPRs can be laterally segregated along continuous membranes, we occasionally observed DAB-positive compartments in which the labeling of the two receptors was clearly segregated (Fig. 7 *B*).

We also used this approach to investigate whether the subpopulations of dense vesicles enriched for either CD-MPR or ASGPR as shown in Fig. 5 were indeed derived from endosomes. Double immunolabeling of the isolated organelles for the CD-MPR and ASGPR (Fig. 7 *C*) showed within these fractions small DAB-positive vesicles that were either enriched in CD-MPR or in ASGPR label. These data indicate that the CD-MPR and ASGPR are sorted into different subpopulations of endosomal ATV. The application of this approach to study the distribution of receptors and cytosolic factors is under current investigation.

Relative Distribution of the CD-MPR and CI-MPR in Endosomes of BHK Cells Expressing the Human Receptors

The proportions of CD-MPR and CI-MPR present in TGR and endosomes of HepG2 cells differ from values published for NRK cells (Griffiths et al., 1990). In these cells >90% of the CI-MPR label was found in endosomes, and <1% in the TGR. To investigate the possibility that HepG2 cells display an exceptional rather than a general distribution pattern, we extended our studies to BHK cells which were cotransfected with the human cDNAs encoding for the CD-MPR and CI-MPR (Chao et al., 1990). Endosomes were identified by the presence of internalized BSA-gold. Analogous to the HepG2 cells, labeling for both receptors was found within the endosomes (Fig. 8), TGR, cytoplasmic vesicles, and at the plasma membrane (not shown). Both MPRs were found within the same endosomes. As was the case with Tf-HRP in HepG2 cells, labeling with BSA-gold did not allow a reliable differentiation between different types of endosomes in these cells. Already after 3 min of uptake we found BSA-gold within all MPR-containing endosomes. The ultrastructure of MPR containing endosomes in BHK cells was much more variable than in HepG2 cells (see also Griffiths et al., 1989), which prevented us from making an analogous distinction between two subsets of endosomes.

Semi-quantitative analysis of the subcellular distributions of the two MPRs showed that more of both MPRs was present in endosomes of BHK cells than in HepG2 cells (Table V). Of the CD-MPR, 18.5% and of the CI-MPR, 10.5% were present in the TGR. The typical cytoplasmic electron-dense vesicles now provided the main site of label for the CD-MPR (36%). As in HepG2 cells twice as much of CD-MPR than CI-MPR label was found in these cytoplasmic vesicles. Semiquantitative analysis of the relative distribution of the two receptors over the distinct endosomal subcompartments (central vacuole and ATV) revealed that 41% of the CD-MPR and 14.5% of CI-MPR was present in the ATV, indicating an enrichment of the CD-MPR over the CI-MPR in the ATV of 2.8 and, when compared with the central vacuole, of 4. These data are consistent with those in HepG2 cells and indicate that the differential distribution of the two MPRs over the endosomal subcompartments is not a cell type–specific phenomenon and that TGR contains a significant pool of the cell's MPRs.

Table V. Subcellular Distribution of the CD and CI-MPR in Cryosections of BHK Cells Transfected with the Human cDNAs for the Two Receptors

	Percent CD-MPR ± SEM	Percent CI-MPR ± SEM
TGR	18.5 ± 1.5	10.5 ± 2.5
Golgi stack	1.0 ± 0.0	0.0 ± 0.0
Endosomes	28.0 ± 4.0	34.0 ± 2.0
Cytoplasmic vesicles	36.0 ± 5.0	19.0 ± 2.0
Plasma membrane and coated pits	6.5 ± 1.5	13.0 ± 2.0
Rest	9.5 ± 0.5	23.0 ± 4.0

Endosomes were marked with internalized BSA-gold. The numbers of gold particles over the different cell compartments are expressed as percentage of the totals counted for each MPR and represent the mean of two separate quantitations in different grids. In total, 2,169 gold particles representing the CD-MPR and 2,400 gold particles representing the CI-MPR were encountered.

Discussion

In this paper we directly compared the subcellular distributions of the CD-MPR and the CI-MPR by means of double immunolabeling. Only such a morphological approach can answer the question whether the two MPRs reside together within the same structures and also allows measuring of the relative occurrence of the two receptors within a particular structure. We performed our studies in the human hepatoma cell line HepG2 and in BHK cells cotransfected with the cDNAs for the human CD-MPR and CI-MPR. In both cell lines the CD-MPR and CI-MPR colocalized to the TGR, endosomes, cytoplasmic vesicles, and the plasma membrane. A compartment that labeled for one of the MPRs exclusively was not found. These observations are in agreement with the work of Messner et al. (1989), who studied the distribution

Figure 8. Immunolabeling of the CD-MPR and CI-MPR in endosomes of BHK cells cotransfected with the cDNAs encoding the human receptors. Both MPRs are present in endosomes (★) which were identified by the presence of internalized BSA-5 nm gold (*A–C*) CD-MPR (10 nm gold). (*D–F*) CI-MPR (10 nm gold). (*G*) Double immunolabeling of the CD-MPR (10 nm gold) and the CI-MPR (15 nm gold). Note that colocalization of endocytosed BSA-5 nm gold with either receptor in the dense typical electron-dense ATV (*arrowheads*) only rarely occurs. Bars, 0.1 μm.

of the two MPRs in bovine liver cells and, using cell fractionation and immunoabsorption, concluded that they codistribute.

In the TGR triple immunolabeling showed that CD-MPR and CI-MPR codistributed and concentrated to the same extent in the same HA I-coated buds. Hence, the two types of MPR provide the first example of two different proteins that concentrate in the same, specialized area of the TGR. This finding is of apparent interest with respect to elucidating the role of the formation of protein–lipid clusters in TGR sorting (Simons and Van Meer, 1988). In view of receptor trafficking their codistribution to HA I-coated buds and vesicles strongly suggests that en route to the endosomes the two MPRs use a common exit from the TGR.

Semiquantitative analysis of the immunogold labeling in cryosections of both HepG2 and BHK cells showed that a considerable percentage of total label of the two MPRs is present in the TGR: 37.3% of CD-MPR and 39.6% of CI-MPR label in HepG2 cells, and 18.5% of CD-MPR and 10.5% of CI-MPR in BHK cells. Respectively, 14.3 and 22.3% of total CD-MPR and CI-MPR label was present within endosomes of HepG2 cells and 28 and 34%, respectively, in the endosomes of BHK cells. These data differ from those published for NRK cells (Griffiths et al., 1990), in which over 90% of CI-MPR was found in endosomes. Our results indicate that the steady-state distribution of MPR in TGR and endosomes may vary between different cell types and that TGR can contain a considerable part of the intracellular MPR pool.

We have chosen for ultrastructural criteria to distinguish two subsets of endosomes. Many morphological studies on different cell types have shown that endosomes containing numerous internal vesicles within the central vacuole are at a relatively late stage in the endocytic pathway. It was postulated by Hopkins et al. (1990) that by a process of "microautophagy" endosomes gradually accumulate internal vesicles until they are eventually loaded with internal membranes. Uptake of endocytotic markers illustrated that the bulk of markers reaches these type of endosomes only after prolonged periods of endocytosis (e.g., Jost et al., 1991; Klumperman et al., 1991; Livne and Oliver, 1986; Mommaas-Kienhuis et al., 1985). Also, functional differences exist between morphologically defined subsets of endosomes. It was found that endosomes containing abundant internal vesicles do not harbor the insulin-regulatable glucose transporter before its translocation to the plasma membrane, whereas empty vacuoles did (Slot et al., 1991). Endosomes in HepG2 cells resembled those as described earlier and we therefore tentatively distinguished early and late endosomes on the basis of a number of internal vesicles. In contrast, we found the endosomal population in BHK cells too diverse to be categorized in a similar way. The exogenous tracers Tf-HRP and BSA-gold endocytosed for as short as 3 min were found to be present in both subsets of endosomes. This observation may reflect an incomplete block of endocytosis after addition of the fixative. More likely, however, it illustrates that endocytosed material can directly be transported to late endosomes (Stoorvogel et al., 1991; Van Deurs, B., personal communication).

A striking difference in the localization patterns of the two MPRs in both HepG2 and BHK cells was the relative prevalence of the CD-MPR in a population of small cytoplasmic vesicles with a characteristic electron-dense content. These profiles provided an important site of CD-MPR label. Morphologically these cytoplasmic vesicles closely resembled endosomal ATV and there may well be an overlap between these two categories. Also, the relative distribution of the two MPRs over the endosomal central vacuoles and ATV differed markedly. The CD-MPR was found to concentrate in the ATV, whereas the CI-MPR was more prominent in the central vacuole. In early endosomes this resulted in a relative enrichment of the CD-MPR in the ATV as compared with the central vacuole with a factor of 4.5. In late endosomes this factor amounted to 7.8. In BHK cells cotransfected with the human cDNAs encoding the two MPR species, a similar difference in the relative distribution between ATV and central vacuoles was found.

The endosomal ATV may represent vesicles that are in a process of either fusion with or detaching from endosomes. Possible fusogenic vesicles may derive from endocytosis or from the TGR. Our data show that in both HepG2 and BHK cells CD-MPR enriched ATV only occasionally contained endocytotic tracer. Thus, these vesicles probably do not derive directly from endocytosis. ATV are probably also not TGR-derived transport vesicles headed to fuse with endosomes, since in the HA I-positive coated buds and vesicles at the TGR CD-MPR was not enriched over CI-MPR. We therefore favor the idea that the CD-MPR–enriched ATV are the structures that mediate receptor sorting from endosomes for recycling (Geuze et al., 1983, 1987, 1988). Both CD-MPR and CI-MPR are known to recycle between endosomes and TGR (Draper et al., 1990; Duncan and Kornfeld, 1988; Goda and Pfeffer, 1988), but may in part be transported to the plasma membrane. That the CD-MPR–enriched ATV would mediate this latter route is unlikely in view of the results obtained for the double-immunolabeling studies with ASGPR and rab4. The ASGPR, which is an established endosome to plasma membrane recycling receptor, colocalized with CD-MPR in ATV only to a limited extent. Recent studies (Sluys et al., 1992) indicated a regulatory role for rab4 in the recycling of Tf-receptors from (early) endosomes. We now localized rab4 for the first time at the subcellular level to endosomal ATV in HepG2 cells. Quantitative analysis further revealed that only a small subpopulation of endosomal ATV contained CD or CI-MPR as well as rab4, probably representing vesicles en route to the plasma membrane. Our results support the notion that endosomal ATV are important in sorting at the endosomal level and strongly suggest that MPR containing ATV carry MPRs from endosomes to the TGR, the most important target for MPR recycling vesicles.

The enrichment of CD-MPR over CI-MPR in ATV that retrieve the MPRs from the endosomes should lead to a relative enrichment of the CI-MPR in late endosomes. Our semiquantitative data indeed show that in HepG2 cells the CI-MPR is enriched over the CD-MPR in endosomes that we classified as late. An alternative explanation for this phenomenon is that Golgi-derived CI-MPR, more than CD-MPR, can deliver their ligands directly to late endosomes (for review see Kornfeld and Mellman, 1989). However, considering that the two MPRs most likely use a common exit at the TGR, because of their exclusive colocalization in HA I-positive coated buds at the TGR, their targeting to two different populations of endosomes seems unlikely. Also,

evidence is accumulating that substantial levels of the CI-MPR enter the endosomal pathway in a relatively early stage (Stoorvogel et al., 1991; Ludwig et al., 1991) and that lysosomal precursors can be recovered from early endosomes (Ludwig et al., 1991; Rijnboutt et al., 1992). The accumulation of CI-MPR in late endosomes may therefore reflect a relatively slow retrieval of the CI-MPR from maturing endosomes.

In contrast to our observations, Matovcik et al. (1990), who investigated the distribution of the CD-MPR by the immunoperoxidase technique in clone 9 hepatocytes and NRK cells, found the CD-MPR label to be restricted to the TGR. Only when cells were cultured in the presence of weak bases, label for the CD-MPR was detected in endosomes. This discrepancy might be explained by experimental differences or by different culture conditions. Our study suggests that CD-MPR normally occur in endosomes. Separate studies in our laboratory showed CD-MPR present in endosomes of mouse L-cells transfected for the human CD-MPR, rat alveolar type II cells (W. Voorhout, W., personal communication) and mouse macrophages (Harding and Geuze, 1992).

A putative mechanism to trigger the segregation of MPR into the endosomal ATV is ligand dissociation (Braulke et al., 1987; Brown et al., 1984; Gonzalez-Noriega et al., 1980). However, the relation between ligand occupancy and MPR recycling is not clear. Depletion of ligands or free receptors was indeed found to affect the steady state distribution of the CI-MPR (Brown et al., 1984; Gonzalez-Noriega et al., 1980; Geuze et al., 1985), but other studies indicated that the recycling itinerary as such was not changed (Braulke et al., 1987; Brown, 1990; Pfeffer, 1987). The CD-MPR was found to accumulate at its putative delivery site when the dissociation of ligand was prevented by weak bases (Matovcik et al., 1990). On the other hand, weak bases did not induce an enhanced secretion of cathepsin D in cells that lack the CI-MPR (Braulke et al., 1988). Optimal binding to the CD-MPR occurs only at a narrow pH range, but the two types of MPR release their ligands at a similar pH (Hoflack and Kornfeld, 1985*a*,*b*; Hoflack et al., 1987). However, other factors within the endosomal environment, e.g., the presence of cations (Hoflack and Kornfeld, 1985*a*,*b*) or the number of receptors present (Watanabe et al., 1990), may cause the possible more rapid dissociation of ligands from the CD-MPR.

The lateral segregation of the two MPRs within endosomes may also be regulated by intrinsic factors independent of ligand occupancy; e.g., for CD-MPR, alteration of the oligomeric state may affect its recycling kinetics (Waheed and von Figura, 1990). Signals for differential sorting of the two MPRs may, for instance, reside in their cytosolic domains, which do not show significant sequence homologies. On the other hand, the lumenal or transmembrane domain of the CI-MPR have been postulated to play a role for intracellular trafficking of the receptor (Dintzis and Pfeffer, 1990). Whether the lumenal or transmembrane domain are specifically involved in differential sorting within endosomal membranes is not known to date.

Taken together our results suggest that the two types of MPR exit the TGR via the same HA I–decorated vesicles and consequently deliver their ligands to the same subsets of endosomes. The enrichment of the CD-MPR in endosomal ATV as compared to central vacuoles and the predominance of CI-MPR in late endosomes suggest that upon arrival in the endosomes the CD-MPR is more efficiently retrieved into the ATV. The limited colocalization of the CD-MPR and the ASGPR or rab4 within the ATV indicates that the CD-MPR containing ATV are targeted to the TGR rather than to the plasma membrane.

We thank T. Van Rijn, M. Niekerk, and R. Scriwaneck for the preparation of the electronmicrographs. J. W. Slot is indebted for his valuable comments on the manuscript.

Received for publication 17 August 1992 and in revised form 12 March 1993.

References

Ahle, S., A. Maun, U. Eichselbacher, and E. Ungewickell. 1988. Structural relationship between clathrin assembly protein from the Golgi and the plasma membrane. *EMBO (Eur. Mol. Biol. Organ.) J.* 7:919–929.

Bleekemolen, J. E., M. Stein, K. von Figura, J. W. Slot, and H. J. Geuze. 1988. The two mannose 6-phosphate receptors have almost identical subcellular distributions in U937 monocytes. *Eur. J. Cell Biol.* 47:366–372.

Braulke, T., C. Gartung, A. Hasilik, and K. von Figura. 1987. Is movement of mannose 6-phosphate-specific receptor triggered by binding of lysosomal enzymes? *J. Cell Biol.* 104:1735–1742.

Braulke, T., M. Stein, T. Marquardt, C. Gartung, A. Hasilik, and K. von Figura. 1988. Receptor-dependent transport of lysosomal enzymes. *Indian J. Biochem. Biophys.* 25:95–101.

Brown, W. J. 1990. Cation-independent mannose 6-phosphate receptors are concentrated in trans Golgi elements in normal human and I-cell disease fibroblasts. *Eur. J. Cell Biol.* 51:201–210.

Brown, W. J., E. Constantinescu, and M. Gist Farquhar. 1984. Redistribution of mannose 6-phosphate receptors induced by tunicamycin and chloroquine. *J. Cell Biol.* 99:320–326.

Brown, W. J., J. Goodhouse, and M. Gist Farquhar. 1985. Mannose 6-phosphate receptors for lysosomal enzymes cycle between the Golgi-complex and endosomes. *J. Cell Biol.* 103:1235–1247.

Chao, H., A. Waheed, R. Pohlman, A. Hille, and K. von Figura. 1990. Mannose 6-phosphate receptor dependent secretion of lysosomal enzymes. *EMBO (Eur. Mol. Biol. Organ.) J.* 9:3507–3513.

Dintzis, S. M., and S. R. Pfeffer. 1990. The mannose 6-phosphate receptor cytoplasmic domain is not sufficient to alter the cellular distribution of a chimeric EGF-receptor. *EMBO (Eur. Mol. Biol. Organ.) J.* 9:77–84.

Draper, R. K., Y. Goda, F. M. Brodsky, and S. R. Pfeffer. 1990. Antibodies to clathrin inhibit endocytosis but not recycling to the trans Golgi network in vitro. *Science (Wash. DC).* 248:1539–1541.

Duncan, J. R., and S. Kornfeld. 1988. Intracellular movement of two mannose 6-phosphate receptors: return to the Golgi apparatus. *J. Cell Biol.* 106:617–628.

Geuze, H. J., J. W. Slot, G. J. A. M. Strous, H. F. Lodish, and A. L. Schwartz. 1983. Intracellular site of asialoglycoprotein receptor-ligand uncoupling: double-label immunoelectron microscopy during receptor-mediated endocytosis. *Cell.* 32:277–287.

Geuze, H. J., J. W. Slot, G. J. A. M. Strous, J. Peppard, K. von Figura, A. Hasilik, and A. L. Schwartz. 1984. Intracellular receptor sorting during endocytosis: comparative immunoelectron microscopy of multiple receptors in rat liver. *Cell.* 37:195–204.

Geuze, H. J., J. W. Slot, G. J. A. M. Strous, A. Hasilik, and K. von Figura. 1985. Possible pathways for lysosomal enzyme delivery. *J. Cell Biol.* 101:2253–2262.

Geuze, H. J., J. W. Slot, and A. L. Schwartz. 1987. Membranes of sorting organelles display lateral heterogeneity in receptor distribution. *J. Cell Biol.* 104:1715–1723.

Geuze, H. J., W. Stoorvogel, G. J. Strous, J. W. Slot, J. E. Bleekemolen, and I. Mellman. 1988. Sorting of mannose 6-phosphate receptors and lysosomal membrane proteins in endocytic vesicles. *J. Cell Biol.* 107:2491–2501.

Geuze, H. J., J. W. Slot, and A. L. Schwartz. 1992. The trans-Golgi exits of MPR. *In* Hepatic Endocytosis of Lipids and Proteins. E. Windler and H. Greten, editors. W. Zuckschwerdt Verlag, Hamburg. 28–34.

Glickman, J. N., E. Conibear, and B. M. F. Pearse. 1989. Specificity of binding of clathrin adaptor to signals in the mannose 6-phosphate/insulin-like growth factor II receptor. *EMBO (Eur. Mol. Biol. Organ.) J.* 8:1041–1047.

Goda, Y., and S. R. Pfeffer. 1988. Selective recycling of the mannose 6-phosphate/IGF-II receptor to the trans Golgi network in vitro. *Cell.* 55:309–320.

Gonzalez-Noriega, A., J. H. Grubb, V. Talkad, and W. S. Sly. 1980. Chloroquine inhibits lysosomal enzyme pinocytosis and enhances lysosomal enzyme secretion by impairing receptor recycling. *J. Cell Biol.* 85:839–852.

Griffiths, G., R. Back, and M. Marsh. 1989. A quantitative analysis of the endocytic pathway in baby hamster kidney cells. *J. Cell Biol.* 109:2703–2720.

Griffiths, G., R. Matteoni, R. Back, and B. Hoflack. 1990. Characterization of the cation-independent mannose 6-phosphate receptor-enriched

prelysosomal compartment in NRK cells. *J. Cell Sci.* 95:441–461.

Harding, C. V., and H. J. Geuze. 1992. Class II MHC molecules are present in macrophage lysosomes and phagolysosomes that function in the phagocytic processing of Listeria monocytogenes for presentation to T cells. *J. Cell Biol.* 119:531–542.

Hoflack, B., and S. Kornfeld. 1985*a*. Lysosomal enzyme binding to mouse P388D1 macrophage membranes lacking the 215-kDa mannose 6-phosphate receptor: Evidence for the existence of a second mannose 6-phosphate receptor. *Proc. Natl. Acad. Sci. USA.* 82:4428–4432.

Hoflack, B., and S. Kornfeld. 1985*b*. Purification and characterization of a cation-dependent mannose 6-phosphate receptor from murine P288D$_1$ macrophages and bovine liver. *J. Biol. Chem.* 260:12008–12014.

Hoflack, B., K. Fulimoto, and S. Kornfeld. 1987. The interaction of phosphorylated oligosaccharides and lysosomal enzymes with bovine liver cation-dependent mannose 6-phosphate receptor. *J. Biol. Chem.* 1:123–129.

Hopkins, C. R., A. Gibson, M. Shipman, and K. Miller. 1990. Movement of internalized ligand-receptor complexes along a continuous endosomal reticulum. *Nature (Lond.).* 346:335–339.

Jin, M., G. G. Sahagian, and M. D. Snider. 1989. Transport of surface mannose 6-phosphate receptor to the Golgi-complex in cultured human cells. *J. Biol. Chem.* 264:7675–7680.

Jost, C. R., R. De Goede, J. A. M. Fransen, M. R. Daha, and L. A. Ginsel. 1991. On the origin of the FCRIII (CD16)-containing vesicle population in human neutrophil granulocytes. *Eur. J. Cell Biol.* 54:313–321.

Junghans, U., A. Waheed, and K. von Figura. 1988. The 'cation dependent' mannose 6-phosphate receptor binds ligands in the absence of divalent cations. *FEBS (Fed. Eur. Biochem. Soc.) Lett.* 237:81–84.

Kiess, W., G. D. Klickenstaff, M. M. Sklar, C. L. Thomas, S. P. Nissley, and G. G. Sahagian. 1988. Biochemical evidence that the type II insulin-like growth factor receptor is identical to the cation-independent mannose 6-phosphate receptor. *J. Biol. Chem.* 263:9339–9344.

Klumperman, J., J. C. Boekestijn, A. M. Mulder, J. A. M. Fransen, and L. A. Ginsel. 1990. Intracellular localization and endocytosis of brush border enzymes in the enterocyte-like cell line Caco-2. *Eur. J. Cell Biol.* 54:76–84.

Kornfeld, S., and I. Mellman. 1989. The biogenesis of lysosomes. *Annu. Rev. Cell Biol.* 5:483–525.

Livne, E., and C. Oliver. 1986. Internalization of cationized ferritin by isolated pancreatic acinar cells. *J. Histochem. Cytochem.* 34:167–176.

Ludwig, T., G. Griffiths, and B. Hoflack. 1991. Distribution of newly synthesized lysosomal enzymes in the endocytic pathway of normal rat kidney cells. *J. Cell Biol.* 115:1561–1572.

Marsh, M., G. Griffiths, G. E. Dean, I. Mellman, and A. Helenius. 1986. Three-dimensional structure of endosomes in BHK-21 cells. *Proc. Natl. Acad. Sci. USA.* 83:2899–2903.

Matovcik, L. S., J. Goodhouse, M. Gist Farquhar. 1990. The recycling itinerary of the 46 kDa mannose 6-phosphate receptor—Golgi to late endosomes—coincides with that of the 215 kDa M6PR. *Eur. J. Cell Biol.* 53:203–211.

Messner, D. J., G. Griffiths, and S. Kornfeld. 1989. Isolation and characterization of membranes from bovine liver which are highly enriched in mannose 6-phosphate receptors. *J. Cell Biol.* 108:2149–2162.

Mommaas-Kienhuis, A. M., L. H. Krijbolder, V. W. M. Van Hinsbergh, W. Th. Daems, and B. J. Vermeer. 1985. Visualization of binding and receptor-mediated uptake of low density lipoproteins by human endothelial cells. *Eur. J. Cell Biol.* 36:201–208.

Morgan, D. O., J. C. Edman, D. N. Standing, V. A. Fried, and M. C. Smith. 1987. Insulin-like growth factor II receptor as a multifunctional binding protein. *Nature (Lond.).* 329:301–307.

Pfeffer, S. 1987. The endosomal concentration of a mannose 6-phosphate receptor is unchanged in the absence of ligand synthesis. *J. Cell Biol.* 105:229–234.

Rijnboutt, S., W. Stoorvogel, H. J. Geuze, and G. J. Strous. 1992. Identification of subcellular compartments involved in the biosynthetic processing of cathepsin D. *J. Biol. Chem.* 267:15665–15672.

Sahagian, G. G., J. Distler, and G. W. Jourdian. 1981. Characterization of a membrane-associated receptor from bovine liver that binds phosphomannosyl residues of bovine testicular β-galactosidase. *Proc. Natl. Acad. Sci. USA.* 78:4289–4293.

Schwartz, A. L. 1984. The Hepatic asialoglycoprotein receptor. *Crit. Rev. Biochem.* 16:207–233.

Simons, K., and G. Van Meer. 1988. Lipid sorting in epithelial cells. *Biochemistry.* 27:6197–6202.

Slot, J. W., H. J. Geuze, and A. J. Weerkamp. 1988. Localization of macromolecular components by application of the immunogold technique on cryosectioned bacteria. *Methods Microbiol.* 20:211–236.

Slot, J. W., H. J. Geuze, S. Gigengack, G. E. Lienhard, and D. E. James. 1991. Immunolocalization of the insulin regulatable glucose transporter in brown adipose tissue of the rat. *J. Cell Biol.* 113:123–135.

Sluys, P. v. d., M. Hull, P. Webster, P. Male, B. Goud, and I. Mellman. 1992. The small GTP-binding protein rab4 controls an early sorting event on the endocytic pathway. *Cell.* 70:729–740.

Stein, M., J. E. Zijderhand-Bleekemolen, H. Geuze, A. Hasilik, and K. von Figura. 1987*a*. Mr 46,000 mannose 6-phosphate specific receptor: its role in targeting of lysosomal enzymes. *EMBO (Eur. Mol. Biol. Organ.) J.* 6: 2677–2681.

Stein, M., T. Braulke, C. Krentler, A. Hasilik, and K. von Figura. 1987*b*. 46-kDa mannose 6-phosphate receptor: Biosynthesis, processing, subcellular location and topology. *Biol. Chem. Hoppe-Seyler.* 368:937–947.

Stoorvogel, W., H. J. Geuze, and G. J. Strous. 1987. Sorting of endocytosed transferrin and asialoglycoprotein occurs immediately after internalization in HepG2 cells. *J. Cell Biol.* 104:1261–1268.

Stoorvogel, W., H. J. Geuze, J. M. Griffith, and G. J. Strous. 1988. The pathways of endocytosed transferrin and secretory protein are connected in the trans Golgi reticulum. *J. Cell Biol.* 106:1821–1829.

Stoorvogel, W., G. J. Strous, H. J. Geuze, V. Oorschot, and A. L. Schwartz. 1991. Late endosomes derive from early endosomes by maturation. *Cell.* 65:417–427.

Tong, P. Y., and S. Kornfeld. 1989. Ligand interactions of the cation-dependent mannose 6-phosphate receptor. *J. Biol. Chem.* 264:7970–7975.

Waheed, A., and K. von Figura. 1990. Rapid equilibrium between monomeric, dimeric and tetrameric forms of the 46-kDA mannose 6-phosphate receptor at 37°C. Possible relation to the function of the receptor. *Eur. J. Biochem.* 193:47–54.

Watanabe, H., J. E. Grubb, and W. S. Sly. 1990. The overexpressed human 46-kDa mannose 6-phosphate receptor mediates endocytosis and sorting of β-glucuronidase. *Proc. Natl. Acad. Sci. USA.* 87:8036–8040.